Handai Nanophotonics, Volume 2
S. Kawata and H. Masuhara (Editors)

Chapter 1

Magnetic plasmon resonance

A. K. Sarychev[a], G. Shvets[b], and V. M. Shalaev[c]

[a]Ethertronics Inc., San Diego, CA 92121,

[b]Department of Physics, The University of Texas at Austin, Austin, TX 78712

[c]School of Electrical and Computer Engineering, Purdue University, West Lafayette, IN 47907

The optical properties of nanostructured metamaterials have been intensively studied during the last decade. It has been proposed by Pendry, who further developed earlier studies on negative refraction [1,2] that a metamaterial with negative dielectric permittivity ε and negative magnetic permeability μ could be used for developing a super-lens providing a sub-wavelength resolution. According to Pendry, when the scattered light passes through a material with a negative refractive index (specifically, when $n=\sqrt{\varepsilon\mu}=-1$ and the two impedances are matched), the evanescent components of the scattered field grow exponentially, allowing the restoration of the scattered image with subwavelength resolution. Smith, Padilla, Vier, and Shultz [3] have demonstrated negative-refraction materials in the microwave range. These materials are also referred to as double-negative or left-handed materials (LHMs), because the electric field and magnetic field along with the wavevector form a left-handed system in this case. In addition to super resolution, the unusual and sometimes counter-intuitive properties of LHMs make them very promising for applications in resonators, waveguides and other microwave and optical elements (see [4] and [5-7]). Huge enhancement of the local em field, accompanying the subwavelength resolution, can be used to enhanced Raman and nonlinear spectroscopy of atoms and molecules distributed over the surface of a LHM.

In spite of large efforts LHMs have not been demonstrated yet in the optical range. To obtain a negative refraction in the optical range, one needs to have a metamaterial with optical magnetism, which is a challenging problem because magnetism is typically weak in the high-frequency range. Relaxation

times of paramagnetic and ferromagnetic processes are long in comparison with the optical period and collective magnetic responses become small at high frequencies. With no collective effects, the magnetic susceptibility is very small since it is proportional to $v^2/c^2 \approx \beta^2 \approx 10^{-4}$, where v is the velocity of electron in atom, c is the speed of light, and $\beta = e^2/hc \cong 1/137$. [This is because the ratio v/c appears first with the magnetic field **H** in the interaction Hamiltonian and again in the magnetic moment **M** of atoms.]

For microwave LHMs artificial magnetic elements such as split-ring resonators (SPRs) and Swiss roll structures have been proposed and experimentally implemented [3, 4, 8]. In the microwave part of the spectrum metals can be considered as perfect conductors because the skin depth is much smaller than the metallic feature size. In the optical part of the spectrum, however, thin (sub-wavelength) metal components behave very differently because their sizes become comparable to the skin depth. This is the physical reason preventing the transfer of the approaches used in design of microwave LHMs to the optical range. By proper accounting for the metal properties in the optical range (finite $\varepsilon < 0$), we demonstrate that the artificial magnetism can exist in (sub-wavelength) plasmonic structures. Artificial magnetism is caused by the magnetic plasmon resonance (MPR), which is primely determined by the geometry and material properties of the structure and to a lesser degree, by the ratio of the structure size and radiation wavelength λ.

Previously we proposed optical LHMs based on half-wavelength-long metal rods so that a magnetic resonance in this case was directly related to the wavelength [4, 9]. Here we show that MPR can occur in structures much smaller than the wavelength. Moreover, there is a close analogy between the electrical surface plasmon resonance (SPR) and MPR. The electrical SPR occurs in the optical and infrared part of the spectrum and results from a collective electron oscillation in metal structures. Consider, for example, an elliptical metal particle that has the electrical dipole polarizability $\alpha_E \propto \left[1+\gamma(\varepsilon_m - 1)\right]^{-1}$, where ε_m is the metal permittivity and $\gamma < 1$ is the depolarization factor, which depends on the aspect ratio. For "good" optical metals (Ag, Au, Al, etc.), the real part of ε_m is negative and large while its imaginary part is relatively small in the optical range. The plasmon resonance corresponds to the condition $\mathrm{Re}\,\varepsilon_m(\omega) = 1 - 1/\gamma$ and it critically depends on metal properties and the shape of a metal nanoparticle. For particles much smaller than the wavelength, the SPR is size- and wavelength-independent. Many important plasmon-enhanced optical phenomena and applications of metal nanocomposites are based on the electrical SPR (see, for example, [10]).

Below we show that along with the electrical SPR, specially arranged metal nanoparticles can support a MPR, with the resonance frequency ω_r independent

of the size and λ. Such structures act as optical nanoantennas by concentrating large electric and magnetic energies on the nanoscale at the optical frequencies. The magnetic response is characterized by the magnetic polarizability α_M with the resonant behavior similar to α_E: its real part changes the sign near the resonance and becomes negative for $\omega > \omega_r$, as required for LHMs. Similar to the electrical SPR where the optical cross section of a nanostructure with size $a << \lambda$ can be as large as λ^2 the MPR can also be characterized by a large optical cross-section.

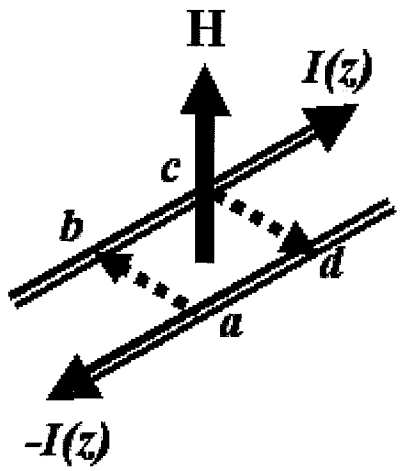

Fig. 1. Currents in the two-wire line excited by external magnetic field **H**. The displacement currents, "closing" the circuit, are shown by dashed lines

We consider first a pair of parallel metal rods. The external magnetic field excites the electric current in the pair of the rods as shown in Fig1. The magnetic moment associated with the circular current flowing in the rods results in a magnetic response of the system. Suppose that an external magnetic field $H = H_0 \exp(-i\omega t)$ is applied perpendicular to the plane of the pair. The circular current $I(z)$ excited by the magnetic field flows in opposite directions in the nanowire pair, as shown in Fig. 1. The displacement currents flowing between the nanowires close the circuit. We introduce the electric potential $U(z) = \int_a^b \mathbf{E}d\mathbf{l}$ between the pair where the integration is along the line $\{a(z), b(z)\}$. To find the current $I(z)$, we integrate the Maxwell equation curl $\mathbf{E} = ik(\mathbf{H}_0 + \mathbf{H}_{in})$ over the contour {*a, b, c,* d} in Fig. 1, where $k = \omega/c$ and $\mathbf{H}_{in}$ = curl **A** is the magnetic field induced by the current. It is assumed that the nanowire length $2a$ is much larger than the distance d between the nanowires

and the radius of a nanowire $b \ll d$. We also assume that $kd \ll 1$. Under these assumptions, the vector potential **A** is directed along the nanowires (z direction) and the integration of the Maxwell equation gives

$$\left(IR - ikA_z + dU/dz\right)\Delta = ikH_0 d\Delta z, \tag{1}$$

where the pair impedance $R \approx 2/(\sigma\pi b^2) = 8i/(\varepsilon b^2)$ [$\varepsilon = i4\pi\sigma/\omega$ is the metal permittivity] and $\pm IR/2$ are the electric fields on the surface of the nanowires. The electric potential $U(z)$ between the pair is given by solution of Maxwell's equations that can be written for $a >> d >> b$ as

$$U(z) \cong 2q(z)\int_{-a}^{a}\left(\frac{1}{r_1}-\frac{1}{r_2}\right)dz' + \int_{-a}^{a}\left[\frac{q(z')\exp(ikr_1)-q(z)}{r_1} - \frac{q(z')\exp(ikr_2)-q(z)}{r_2}\right]dz' \tag{2}$$

where $q(z)$ is the electric charge per unit length, $r_1 = \sqrt{(z-z')^2 + b^2}$, $R_2 = \sqrt{(z-z')^2 + h^2}$ and the terms $\sim (b/a)^2$ are neglected. We explicitly separate in Eq. (2) the first term, which has a singularity when $b \to 0$; it can be estimated as $4q(z)\ln(d/b)$. The second term in Eq. 2 is regular for $b \to 0$ and we can expand it over $d/a << 1$. Thus we obtain a local relation between U and q: $U(z) = Cq(z)$, where $C = \left[4\log(d/b) - 3(d/a)^2 + (dk)^2(2\log(2a/d) - 1)/2\right]^{-1}$

The vector potential A_z can be found following the same procedure which results in $A_z(z) = (L/c)I(z)$, where the inductance is given by $L - 4\ln(d/b) - (d/a)^2[3 + 4iak + 6\log(2a/d)]/6$. We substitute $U(z)$ and $A_z(z)$ into Eq. (1), taking into account the charge conservation law $kI/dz = i\omega q(z)$, and obtain the second-order differential equation for the current,

$$\frac{d^2 I(z)}{dz^2} = -g^2 I(z) + \frac{Cd\omega^2}{c}H_o \tag{3}$$

where $-a < z < a, I(-a) = I(a) = 0$, and parameter g is given as $g^2 = k^2\left[LC - 8C\left[(kb)^2\varepsilon_m\right]^{-1}\right]$. The product LC can be estimated as $LC \sim 1$. We consider here the "quasistatic" case $|8C[(kb)^2\varepsilon_m]^{-1}| >> 1$ when parameter $G = ag$ depends only on the metal permittivity and aspect ratio:

$$G^2 \approx -2(a/b)^2 \ln(d/b)/\varepsilon_m \tag{4}$$

The case of the strong skin effect ($|(kb)^2\varepsilon_m|^{-1}<<1$, $g \approx k$), when the pair of metal wires has a so-called antenna resonance at $ka = \pi/2$, was numerically simulated in our previous papers [9,11] and in papers by Panina et al. [12].

We solve Eq.(3) for the current *I(z)* and calculate the magnetic moment $\mathbf{m} = (2c)^{-1} \int [\mathbf{r} \times \mathbf{j}(\mathbf{r})] d\mathbf{r}$, where $\mathbf{j}(\mathbf{r})$ is the density of the current and the integration is over the two nanowires as well as over the space between them where the displacement currents are flowing. Thus we obtain

$$m = \frac{1}{2} H_0 a^3 \ln(d/b)(kd)^2 \frac{\tan G - G}{G^3} \tag{5}$$

The metal permittivity ε_m has a large negative value in the optical range while its imaginary part is small; therefore, the magnetic moment m has a resonance at $G \approx \pi/2$ when the moment m attains large values. The magnetic resonance frequency $\omega = \omega_r$ depends on geometry of the system and material properties. In analogy with the electric SPR in metal nanoparticles, we see that for the MPR, the size of the sticks can also be arbitrary small in comparison with the wavelength of the incident light. This is in a striking difference with the previously considered magnetic resonance at $a = \lambda/4$ [9]. For a lossless metal the magnetic polarizability $4\pi(m/H_0)$ goes to $-\infty$ at the resonance. Thus, the MPR opens the possibility for engineering efficient LHM in the optical range.

For a typical metal, the permittivity $\varepsilon_m(\omega)$ can be well approximated by the Drude formula for the red and infrared parts of the spectrum: $\varepsilon_m(\omega) \cong -(\omega/\omega_p)^2/(1 - i\omega_\tau/\omega)$, where ω_p is the plasma frequency and the relaxation parameter is small, $\omega_\tau/\omega << 1$. Then the polarizability α_M normalized to the volume $V = 4abd$ of the pair has the following form near the MPR:

$$\alpha_M = \frac{4\pi m}{H_0 V} = \frac{16ad\omega_p}{\lambda^2 \omega_r \sqrt{2\log(d/b)}} \left[1 - \omega/\omega_r - i\omega_r/(2\omega_r)\right]^{-1} \tag{6}$$

where the resonance frequency $\omega_r = b\pi\omega_p \sqrt{2\log(d/b)}/(4a)$. The plasma frequency ω_p is typically in the ultraviolet part of the spectrum so that $\omega_\tau << \omega_p$ and the pre-factor in Eq. (6) can be on the order of one, even for a nanowire length $2a$ much smaller than the wavelength λ of the incident light, so that a strong MPR can be observed. We can also estimate the optical cross-section for the MPR, $\sigma_M \sim \alpha_M V/\lambda$, assuming that the logarithm factor is ~ 1 and that radiation losses dominate (so that $\omega_\pi \sim \omega V/\lambda^3$); this gives

$\sigma_M \sim a^2(d/b)$. Thus, the magnetic cross-section σ_M can be very large and, in particular, comparable to λ^2 (as in the case of the SPR in spheroids, where $\sigma_E \sim \lambda^2$ despite the fact that all sizes involved are much smaller than the wavelength. Thus, by employing both resonances, SPR and MPR, one can accomplish a strong coupling of nanostructures to both components of light, electrical and magnetic.

We now consider a metal nanoantenna that has a horseshoe\ shape, which is obtained from a pair of nanowires by shorting it at one of the ends (see Fig 2). When the quasistatic condition $|8C[(kb)^2\varepsilon_m]^{-1}|>>1$ holds, the electric current $I(z)$ in a horseshoe nanoantenna can be obtained from Eq. (3) where the boundary condition changes to $I_{z=a} = (dI/dz)_{z=0} = 0$ and, as above, $a >> d >> b$. It is easy to check that the magnetic polarizability α_M is still given by Eq. (6), where a is now equal to the total length of the horseshoe nanoantenna. Therefore, the horseshoe nanoantenna provides the same magnetic polarizability α_M at twice shorter length.

Consider now a magnetic permeability μ for a metamaterial where the horseshoe nanoantennas are oriented in one direction ("z" direction in Fig. 1) and are organized in the periodic square lattice. The tensor μ component, which is in the direction perpendicular to the plane of the sticks (**H** direction in Fig. 1), can be estimated from the Lorenz-Lorentz formula [14] $(\mu_e - 1)/(\mu_e + 1) = p\alpha_M/3$, where p is the volume concentration of the nanoantennas. Results of our calculations of $\mu_e = \mu_1 + i\mu_2$ for silver horseshoe nanoantennas are shown in Fig. 2; the optical parameters for silver were taken from [10, 15]. As one can see in the figure, the negative magnetism can be observed, for example, in the near-infrared part of the spectrum, including the telecommunication wavelength of 1.5 μm. By varying nanoantenna parameters, one can tune the position of the MPR for any frequency in the visible and infrared parts of the spectrum.

For practical applications of the optical magnetism losses may play an important role. We estimate losses (given by μ_2) at the wavelength corresponding to the condition $\mu_1 = -1$ as $\mu_{2r} = \lambda_r^2 \omega_\tau \sqrt{2\log(d/b)}/\left(8\omega_p adp\right)$, where λ_r is the resonance wavelength. For metals at room temperatures losses are significant (for silver, $\mu_{2r} \sim 0.3$, see Fig. 2) but still they are relatively small. These losses can be much smaller at low temperatures and atomic quality of metal crystals. We also note that the radiative losses (which are given by the small imaginary part of the inductance L) are of no importance for nanoantennas arranged in a periodic array (i.e., in a plasmonic crystal); the radiation

corrections, in this case, result in a change in the spatial dispersion rather than in an increase of μ_2.

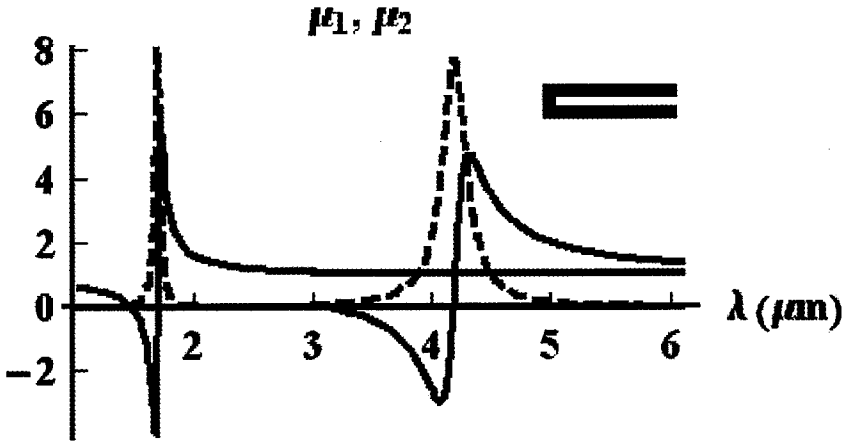

Fig. 2. Optical magnetic permeability $\mu = \mu_1 + \mu_2$ (μ_1 - continuous line, μ_2 - dashed line) of the composite containing $\subset$ shaped silver nanoantennas; volume concentration $p = 0.3$; left curves: $a = 200$ *nm*, $d = 50$ *nm*, $b = 13$ *nm*; right curves $a = 600$*nm*, $d = 90$ *nm*, $b = 13$ *nm*.

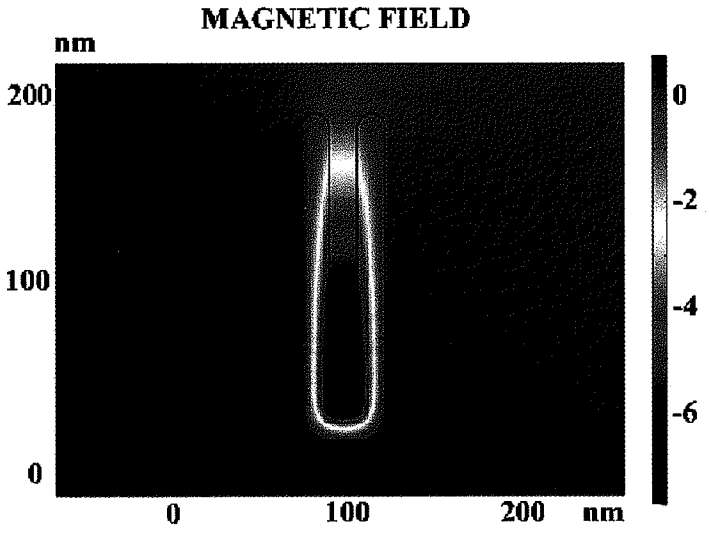

Fig. 3. Magnetic plasmon resonance in silver nanoantenna, which is placed in a maximum of external field H_0 directed perpendicular to the plane; the frequency corresponds to $\lambda = 1.5\mu m$.

The above results can be easily extended to the two-dimensional case where the metal nanoantennas have horseshoe profile in x,y plane and extended to $z = \pm\infty$. The quasistatic case corresponds to the condition $|k^2 bd\varepsilon_m| >> 1$, where b is the thickness of the walls of the horseshoe nanoantenna and d is the distance between the opposite walls. Then the resonance frequency ω_r is defined by the equation $G = 2a\sqrt{-2/(\varepsilon_m bd)} = \pi/2$, where a is the nanoantenna length. In Fig. 3 we show the local magnetic field in the silver nanoantenna that resonates at wavelength $\lambda = 1.5\mu m$.

Near the resonance magnetic field inside the nanoantenna is large in magnitude and it is directed opposite to the external field H_0, which results in negative magnetic permeability. The size of the nanoantenna is much smaller than the wavelength yet the resonance magnetic field is not curl-free since it changes direction at the walls. To estimate the effective magnetic permeability in this case we use the approach developed in Ref. [16]. Thus we obtain $\mu_z = 1 + p(sH_0)^{-1} \int (H_{in} - H_0) ds$ for a plasmonic crystal composed by the nanoantennas, where H_{in} is the magnetic field inside a horseshoe nanoantenna; the integration is over the area $s = da$, and p is a concentration of the nanoantennas organized in a square lattice. Near the resonance we obtain the following equation for $\mu_z = (32/\pi) a^2 p \lambda^{-2} (\pi/2 - G)^{-1}$. For a good optical metal the magnetic permeability has a sharp resonance and can acquire large negative values for $\omega > \omega_r$ as shown in Fig. 4.

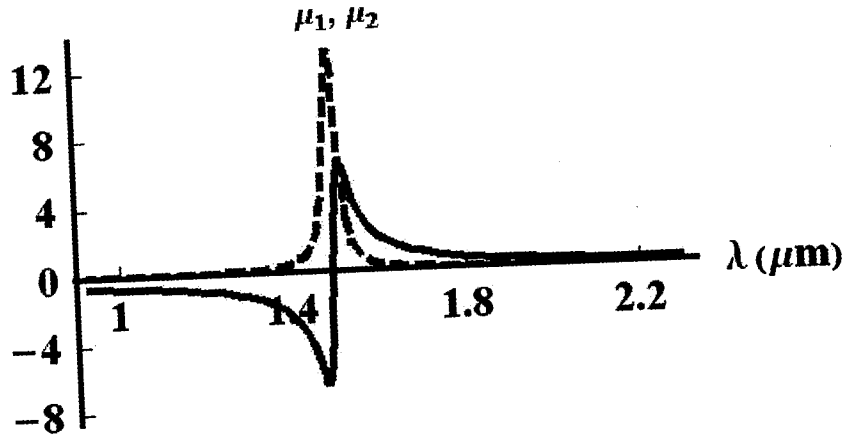

Fig. 4. Optical magnetic permeability $\mu = \mu_1 + \mu_2$ (μ_1 - continuous line, μ_2 - dashed line) of the composite containing silver nanoantennas shown in Fig. 3 organized in square lattice; volume concentration $p = 0.4$.

LHM can be obtained from the horseshoe composite by adding, e.g., metal nanowires as it was done in the microwave case [3]. The horseshoe metamaterial itself can show a left-handed behavior when the nanoantennas are closely packed. We design two-dimensional dense periodic structure consisting of alternative up and down horseshoe nanoantennas. One half of the elementary cell is shown in Fig. 5a. (The structure repeats itself in x and y directions; separation between antenna centers is 80 *nm*). Dispersion relation $\omega(k_x)$ for the electromagnetic wave propagating through the periodic structure in x direction has been calculated by numerically solving the Maxwell's equation for magnetic field H_z. For computational simplicity, we have assumed a hypothetical lossless plasmonic material with the frequency-dependent dielectric permittivity $\varepsilon = 1 - \omega_p^2/\omega^2$, where $2\pi c/\omega_p = 225nm$. The frequency ω and the wavevector k are normalized to $\omega_0 = 2\pi c/\lambda_0$ and $k_0 = 2\pi/\lambda_0$, respectively, where $\lambda_0 = 1.5\mu m$.

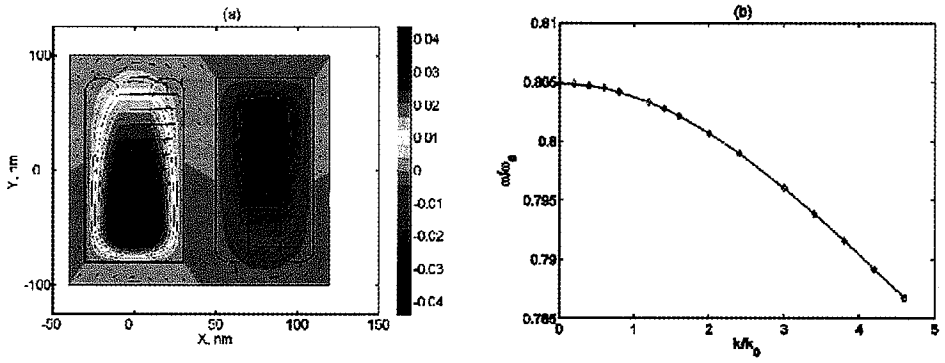

Fig. 5. Plasmonic crystal composed from horseshoe metal nanoantennas; separation between antennas centers 80 nm. Magnetic (color and contours) and electric (arrows) fields inside a periodic array of horseshoe-shaped nanoantennas at the cutoff $k_x = 0$ (b) Dispersion relation ω v.s. k_x for a left-handed electromagnetic wave.

Remarkably, one of the propagating modes (shown in Fig. 5b) exhibits left-handedness: its group velocity $v_{gr} = \partial\omega/\partial k$ opposes its phase velocity. Fig. 5a shows the magnetic field profile and the electric field inside the elementary cell for $k_x = 0$ (magnetic cutoff condition corresponding to $\mu = 0$). Magnetic field is concentrated inside the horseshoes, and has opposite signs in the adjacent horseshoes. The dominant field in the structure is E_x which does not contribute to the Poynting flux in the propagation direction. Electric field is primarily potential (i.e. can be derived from an electrostatic potential), but has a non-vanishing solenoidal component that produces the magnetic field. The fact that

the dominant electric field E_x does not change the sign inside the cell indicates that the mode in question does not owe its negative dispersion to the band-folding effect common in photonic crystals. The left-handed behavior occurs in the vicinity of $\lambda = 1.88\mu m$ which is close to the MPR resonance.

Negative index waves described in this letter occur in plasmonic nanostructures with large negative dielectric permittivity $\varepsilon_m << -1$ and, therefore, they are conceptually different from the negative index waves in perfectly conducting structures [4] and in the structures with $\varepsilon_m \sim -1$ [17].

We considered here two types of nanoantennas that support the MPR in the optical range. Other possible designs could include, for example, nanosized metal spheres sectored into eight equal parts by thin dielectric slits and split-ring resonators (SRRs). The SRRs were successfully used earlier for the microwave LHMs [3]. A subwavelength SRR can provide a large magnetic polarizability at the resonance, when the radius is as follows $R \approx d|\varepsilon_m|/2\pi$, with d being the thickness of the dielectric slit in the ring. However, it seems hard, if not impossible, to have the concentration of SRRs large enough to provide a reasonable negative magnetic permeability in the optical range. Our estimates show that for the optimal concentration, a negative magnetic response of a SRR metamaterial is significantly smaller than for the horseshoe metamaterial considered above. Yet we would like to stress out that SRR metamaterials can have a large paramagnetic response in the optical range (with large and positive μ) with many interesting applications.

In conclusion, we show that a specially designed metal nanoantenna, which is much smaller than the light wavelength, can have a magnetic plasmon resonance (MPR) with the resonant frequency depending on the shape and material properties of the nanoantenna rather than on the wavelength. In this sense, the MPR is similar to the surface plasmon resonance (SPR) in a metal nanoparticle. We show that composites comprising such non-magnetic nanoantennas may have a large magnetic response in the optical spectral range. Metamaterials based on plasmonic nanoantennas supporting both SPR and MPR can have a dielectric permittivity and magnetic permeability, which are simultaneously negative, and thus act as left-handed materials in the optical and infrared spectral ranges.

ACKONWLEDGEMENTS

The authors acknowledge useful contributions and discussions with D. Genov, and V. Podolskiy. This work was supported in part by NSF grants ECS-0210445 and DMR-0121814, and by the ARO MURI W911NF-04-01-0203.

REFERENCES

[1] V. G. Veselago, Soviet Physics Uspekhi, 10 (1968) 509.
[2] J. B. Pendry, Phys. Rev. Lett., 85 (2000) 3966.
[3] D. R. Smith, W. J. Padilla, D. C. Vier, S. C. Nemat-Nasser, and S. Shultz, Phys. Rev. Lett., 84 (2000) 4184.
[4] For recent references see the special issue of Opt. Express, 11 (2003) No 7.
[5] A. A. Houck, J. B. Brock, and I. L. Chuang, Phys. Rev. Lett., 90 (2003) 137401.
[6] C. G. Parazzoli, R. B. Greegor, K. Li, B. E. C. Koltenbah, and M. Tanielian, Phys. Rev. Lett., 90 (2003) 107401.
[7] A. Alu and N. Engheta, IEEE T. Microw. Theory, 52 (2004) 199.
[8] J. B. Pendry, A. J. Holden, D. J. Robbins, and W. J. Stewart, IEEE T. Microw. Theory, 47 (1999) 2075; M. C. K. Wiltshire, J. V. Hajnal, J. B. Pendry, D. J. Edwards, and C. J. Stevens, Opt. Express, 11 (2003) 709.
[9] V. A. Podolskiy, A. K. Sarychev, and V. M. Shalaev, J. Nonlin. Opt. Phys. Mat., 11 (2002) 65; Opt. Express, 11 (2003) 735; A. K. Sarychev, V. P. Drachev, H. K. Yuan, V. A. Podolskiy, and V. M. Shalaev, Proc. SPIE, 5219 (2003) 1.
[11] A. K. Sarychev and V. M. Shalaev, Phys. Rep., 333 (2000) 275.
[12] A. N. Lagarkov and A. K. Sarychev, Phys. Rev. B, 53 (1996) 6318.
[13] L.V. Panina, A. N. Grigorenko, D. P. Makhnovskiy, Phys. Rev. B, 66 (2002) 155411.
[14] D. Landau and E.M. Lifshitz, Electrodynamics of Continuous Media, 2nd ed. Pergamon, Oxford, 1984.
[15] J. D. Jackson, Classical Electrodynamics, J. Wiley & Sons, Inc., 1999.
[16] U. Kreibig and M. Volmer, Optical Properties of Metal Clusters, Springer-Verlag, Berlin, 1995.
[17] A. K. Sarychev, V. M. Shalaev, R. C. McPhedran, Phys. Rev. B, 62 (2000) 8531.
[18] G. Shvets, Phys. Rev. B, 67 (2003) 035109.